Biomedical Journal 47 (2024) 100605

Contents lists available at ScienceDirect

Biomedical Journal

journal homepage: www.elsevier.com/locate/bj

Original Article

Curcumin suppresses RANKL-induced osteoclast precursor autophagy in osteoclastogenesis by inhibiting RANK signaling and downstream JNK-BCL2-Beclin1 pathway

Dianshan Ke [a,b,1], Haoying Xu [b,1], Junyong Han [c,1], Hanhao Dai [a,b,1], Xinwen Wang [d], Jun Luo [a,b], Yunlong Yu [a,b,*], Jie Xu [a,b,**]

[a] Department of Orthopedics, Fujian Provincial Hospital, Fuzhou, Fujian, China
[b] Shengli Clinical Medical College of Fujian Medical University, Fuzhou, Fujian, China
[c] Institute for Immunology, Fujian Academy of Medical Sciences, Fuzhou, Fujian, China
[d] Department of Orthopedics, Dongguan People's Hospital, Southern Medical University, Dongguan, Guangdong, China

ARTICLE INFO

Keywords:
Curcumin
Osteoclast
RANKL
Autophagy
BCL2
Beclin1

ABSTRACT

Background: Curcumin ameliorates bone loss by inhibiting osteoclastogenesis. Curcumin inhibits RANKL-promoted autophagy in osteoclast precursors (OCPs), which mediates its anti-osteoclastogenic effect. But the role of RANKL signaling in curcumin-regulated OCP autophagy is unknown. This study aimed to explore the relationship between curcumin, RANKL signaling, and OCP autophagy during osteoclastogenesis.

Methods: We investigated the role of curcumin in RANKL-related molecular signaling in OCPs, and identified the significance of RANK-TRAF6 signaling in curcumin-treated osteoclastogenesis and OCP autophagy using flow sorting and lentiviral transduction. Tg-hRANKL mice were used to observe the *in vivo* effects of curcumin on RANKL-regulated bone loss, osteoclastogenesis, and OCP autophagy. The significance of JNK-BCL2-Beclin1 pathway in curcumin-regulated OCP autophagy with RANKL was explored via rescue assays and BCL2 phosphorylation detection.

Results: Curcumin inhibited RANKL-related molecular signaling in OCPs, and repressed osteoclast differentiation and autophagy in sorted $RANK^+$ OCPs but did not affect those of $RANK^-$ OCPs. Curcumin-inhibited osteoclast differentiation and OCP autophagy were recovered by TRAF6 overexpression. But curcumin lost these effects under TRAF6 knockdown. Furthermore, curcumin prevented the decrease in bone mass and the increase in trabecular osteoclast formation and autophagy in $RANK^+$ OCPs in Tg-hRANKL mice. Additionally, curcumin-inhibited OCP autophagy with RANKL was reversed by JNK activator anisomycin and TAT-Beclin1 overexpressing Beclin1. Curcumin inhibited BCL2 phosphorylation at Ser70 and enhanced protein interaction between BCL2 and Beclin1 in OCPs.

Conclusions: Curcumin suppresses RANKL-promoted OCP autophagy by inhibiting signaling pathway downstream of RANKL, contributing to its anti-osteoclastogenic effect. Moreover, JNK-BCL2-Beclin1 pathway plays an important role in curcumin-regulated OCP autophagy.

At a glance commentary

Scientific background on the subject:

Curcumin ameliorates bone loss by inhibiting osteoclastogenesis. Curcumin inhibits RANKL-promoted autophagy in osteoclast precursors (OCPs), which mediates its anti-osteoclastogenic effect. But the role of RANKL signaling in curcumin-regulated OCP

Peer review under responsibility of Chang Gung University.

* *Corresponding author*. Department of Orthopedics, Fujian Provincial Hospital, Shengli Clinical Medical College of Fujian Medical University, 134 Dong-Jie Rd., Fuzhou 350001, Fujian, China. Tel.: 0086-0591-88217200.

** *Corresponding author*. Department of Orthopedics, Fujian Provincial Hospital, Fuzhou, 350003, Fujian, China.
E-mail addresses: yuyunlong@fjmu.edu.cn (Y. Yu), jiexud@fjmu.edu.cn (J. Xu).

[1] Dianshan Ke, Haoying Xu, Junyong Han and Hanhao Dai are regarded as co-first authors.

https://doi.org/10.1016/j.bj.2023.100605
Received 25 August 2022; Accepted 8 May 2023
Available online 11 May 2023

autophagy is unknown. This study aimed to explore the relationship between curcumin, RANKL signaling, and OCP autophagy during osteoclastogenesis.

What this study adds to the field:

Our study not only reveals the potential mechanism underlying curcumin-inhibited osteoclast formation, namely the RANK-TRAF6-JNK-BCL2-Beclin1-autophagy signaling pathway, but also provides more evidence for optimizing the application of curcumin in the treatment of osteoclastic osteoporosis.

Bone heath requires a dynamic balance between osteoblastic bone formation and osteoclastic bone resorption. The above balance is destructed due to increased bone resorption activity, and osteoporosis develops from subsequent bone loss and interruptions in the bone microstructure [1,2]. Bone resorption induced by the osteoclast-stimulating factor RANKL is the main pathological basis of osteoporosis [3–5]. Curcumin, extracted from turmeric root, has been reported to treat osteoporosis because it can significantly improve lumbar bone mineral density (BMD) in OVX rats [6]. Therefore, curcumin is a promising plant extract for the treatment of osteoporosis and other osteolytic diseases. Similar results have been reported in various literatures [7–11]. Curcumin is an obvious inhibitor of osteoclastogenesis [10–13]. However, the potential mechanism remains to be further clarified.

As a highly conserved cytoprotective mechanism, autophagy is of great significance for osteoclastogenesis and the bone resorption that it mediates [14–17]. Multiple studies have described that curcumin (including its mimic) functions as an autophagy regulator in a variety of cultured cells. Curcumin attenuates the aging of canine bone marrow mesenchymal stem cells during expansion *in vitro* by activating autophagy [18]. Additionally, curcumin represses (hepatocellular carcinoma) HCC tumor growth by downregulating GPC3/wnt/β-catenin signaling, which is related to autophagy alteration [19]. A novel curcumin analog, EF25-(GSH)2, also induces autophagy in HCC cells [20]. In addition, curcumin promotes autophagic death in human thyroid cancer cells and activates autophagy, preventing cardiomyocyte cell death [21,22]. Current studies show that curcumin is an activator of autophagy, which plays a role in the formation of osteoclasts [11]. Moreover, previous studies have suggested that curcumin directly activates autophagy in OCPs [11]. Even so, curcumin plays a more significant role in inhibiting RANKL-promoted OCP autophagy than in activating autophagy [11]. Curcumin, therefore, contributes to osteoclast formation [11]. Although curcumin suppresses RANKL-promoted OCP autophagy, the underlying mechanism is unknown.

RANKL is the critical stimulator of osteoclastogenesis. There exsit various downstream signaling pathways involved in RANKL-induced osteoclastogenesis, containing MAPK cascades and NF-κB, Akt pathways [23,24]. Furthermore, the RANK-TRAF6 signal axis bridges RANKL and various downstream signals. RANK binds to TRAF6 in response to RANKL stimulation. TRAF6 mutant leads to osteopetrosis due to the missing osteoclastogenic activity [25]. RANK mutation causes the loss of TRAF6-binding site, which could not recover the osteoclastogenic potential of $RANK^{-/-}$ haematopoietic precursors [26]. TRAF6 acts as a key adapter to assemble signaling proteins, resulting in downstream signaling [27–29]. Overall, RANK-TRAF6 signal transduction determines the signal cascades downstream of RANKL. RANKL can upregulate the autophagic activity of OCPs, which also involves multiple downstream pathways related to RANKL [14,30,31]. The regulatory effect of autophagy protein Beclin1 by TRAF6 is also essential for RANKL-induced osteoclastogenesis [32]. So far, whether RANKL downstream signaling mediates curcumin-regulated OCP autophagy still keeps vague.

This study illustrated that curcumin inhibited RANKL-promoted molecular signal transduction in OCPs. Additionally, flow cytometry-related cell sorting and gene transduction techniques were used to learn the significance of RANKL-RANK-TRAF6 signaling in curcumin-regulated OCP autophagy and osteoclast differentiation. Combined with *in vivo* assays, we confirmed that curcumin could suppress OCP autophagy and osteoclastogenesis by inhibiting the RANKL-RANK-TRAF6 signaling. In addition, we further elucidated the significance of JNK-BCL2-Beclin1 signal transduction in curcumin-inhibited OCP autophagy.

Materials and methods

Extraction and induction of OCPs

The tibiae from 4-week-old C57BL/6 J mice (Gem Pharmatech, Nanjing, China) were flushed with α-MEM without FBS. Bone marrow cells were incubated in complete α-MEM (+10% FBS + 100 U/ml penicillin +100 μg/ml streptomycin) for 24 h. Nonadherent cells were cultured on dishes containing M-CSF (30 ng/ml) for 3 days. The collected adherent cells are bone marrow-derived macrophages (BMMs), which can be regarded as OCPs and induced into mature osteoclasts [33]. OCPs were cultured in a humidified environment of 37 °C and 5% CO_2.

Osteoclast induction assays

OCPs (6000 cells/well) were cultured in 96-well plates in α-MEM containing M-CSF (30 ng/ml in all assays) + RANKL (100 ng/ml in all assays) supplemented with other related reagents for 4 days to induce the mature osteoclasts. Osteoclast induction was determined by TRAP staining using a related kit (Sigma–Aldrich) in accordance with manufacturer's protocols. TRAP-positive multinucleate cells (over 3 nuclei) were regarded as mature osteoclasts. TRAP-positive cells over 5 nuclei were regarded as large osteoclasts.

Fluorescence-activated cell sorting (FACS) of OCPs

Rat anti-mouse CD16/32 monoclonal antibody (TruStain FcX™ PLUS, BioLegend, San Diego, CA, USA) was used to block nonspecific binding in treated OCPs or isolated primary bone marrow cells at room temperature for 15 min. PE anti-mouse CD265 (RANK) and CSF1R antibodies (BioLegend) were used to stain cells, and then different clusters of cells were collected on MoFlo XDP flow cytometer (Beckman Coulter). The harvested $RANK^+$ and $RANK^-$ OCPs were cultured in preparation for subsequent experiments. Primary $RANK^+$ $CSF1R^+$ OCPs were directly used for immunofluorescence analysis.

Lentiviral transduction of complementar deoxyribonucleic acid (cDNA) and short hairpin RNA (shRNA)

Lentiviruses encoding TRAF6 cDNA or shRNA targeting TRAF6 (including the corresponding control vector) were constructed by homologous recombination between an expression vector (EX-Puro-Lv105) and cDNA or shRNA in 293 cells using construction kits (GeneCopoeia, MD, USA) in accordance with manufacturer's protocols. After 2 days, viral supernatants were harvested. At a multiplicity of infection (MOI) of 10, OCPs were incubated in the viral fluid containing 8 μg/ml polybrene for 2 days. The infected cells were selected by puromycin (5 μg/ml). The successful transduction was confirmed using Western-Blot analysis.

Western-Blot analyses

The whole cell lysate from indicated OCPs was prepared, packaged into 10% SDS-PAGE gel and transferred to polyvinylidene fluoride membrane (PVDF). Then, the PVDFs were combined with antibodies targeting LC3B (1:1000), p62 (1:1000), NFATc1 (1:1000), DC-stamp (1:1000), phosphorylated (p-)ERK (1:1000), p-JNK (1:1000), p-P38

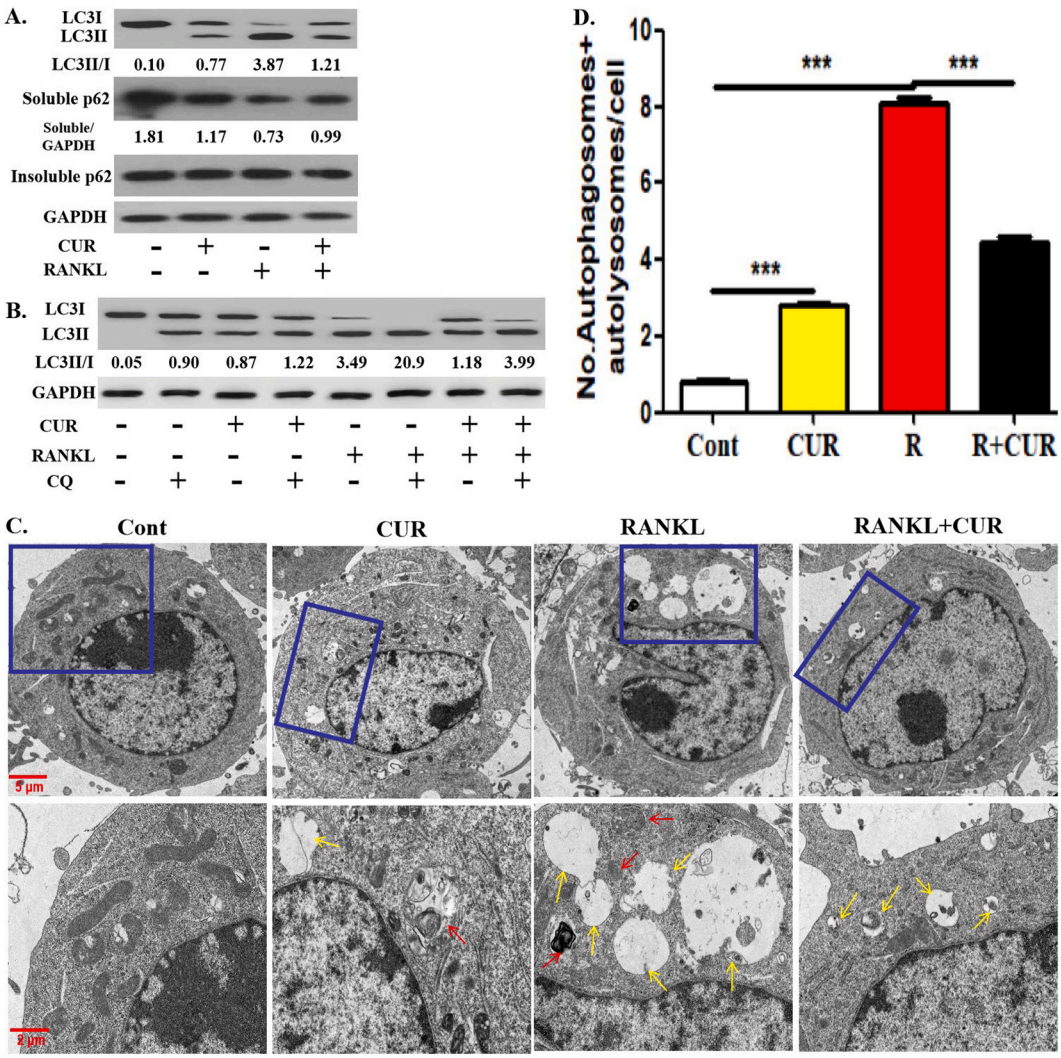

Fig. 1. Curcumin inhibits RANKL-promoted OCP autophagy. (A) After the intervention with 15 μM curcumin or/and RANKL for 12 h, the protein expression levels of LC3 and p62 in OCPs were detected using Western-Blot assays, and LC3 conversion rate was defined as the ratio of LC3II/LC3I. The samples came from the same experiment, and different gels were processed in parallel. (B) After the intervention with 15 μM curcumin or/and RANKL for 12 h in the presence or absence of chloroquine, LC3 protein levels in OCPs were detected using Western-Blot assays, and LC3 conversion rate was defined as the ratio of LC3II/LC3I. The samples came from the same experiment, and different gels were processed in parallel. (C) After the intervention with the above reagents for 2 days, the autophagosomes (red arrows) and autolysosomes (yellow arrows) in OCPs were observed using TEM. Scale bar, 5 or 2 μm. (D) The histogram displays the quantitative results of autophagosomes and autolysosomes in **B** (75 cells from 3 independent experiments). The data are expressed as mean ± SEM from three independent experiments. ***$p <$ 0.001. Cont, control group with PBS only; R, RANKL; CUR, curcumin.

(1:1000), ERK (1:1000), JNK (1:1000), P38 (1:1000), Beclin1 (1:1000) (Cell Signaling Technology, MA, USA), and p-BCL2-S70 (1:1000), p-BCL2-S87 (1:1000), BCL2 (1:1000) (Thermo Fisher Scientific, MA, USA), and PARP (1:1000), Cleaved-PARP (1:1000), Caspase3 (1:3000), Cleaved-Caspase3 (1:5000) (Abcam, Cambridge, UK), and RANK (1:1000), TRAF6 (1:1000) (Santa Cruz Biotechnology, Inc, Texas USA). Horseradish peroxidase (HRP)-linked secondary antibody was used as the secondary antibody. The signals were observed using artificial exposure or a chemiluminescence system (Amersham Image 600, General Electric, MA, USA).

Coimmunoprecipitation assays

According to previous study [34], the preparation of total protein lysate and coimmunoprecipitation analyses were performed. The corresponding antibodies were used for TRAF6 (IP, 1:100; IB, 1:1000), RANK (IP, 1:100; IB, 1:1000) (Santa Cruz Biotechnology) and BCL2 (IP, 1:100; IB, 1:1000), Beclin1 (IP, 1:100; IB, 1:1000), Bax (IP, 1:100; IB, 1:1000) (Thermo Fisher Scientific).

Transmission electron microscopy (TEM) analyses of autolysosomes/ autophagosomes

The preparation, staining and TEM analysis of cell sections were carried out in accordance with manufacturer's protocols. Ultimately, the stained sections were observed by Hitachi 7700 transmission electron microscope (Tokyo, Japan).

Animal experiment

After breeding, 12-weeks-old male Transgenic mice overexpressing RANKL (Tg-hRANKL mice) and littermate wild-type mice were used in this experiment (N = 6–10/group). First, their genotypes were identified by PCR assays. Subsequently, all mice were anesthetized with isoflurane (2%, Inhalation anesthesia), and then sacrificed via cervical dislocation. The mice were considered dead when the heart and breathing stopped.

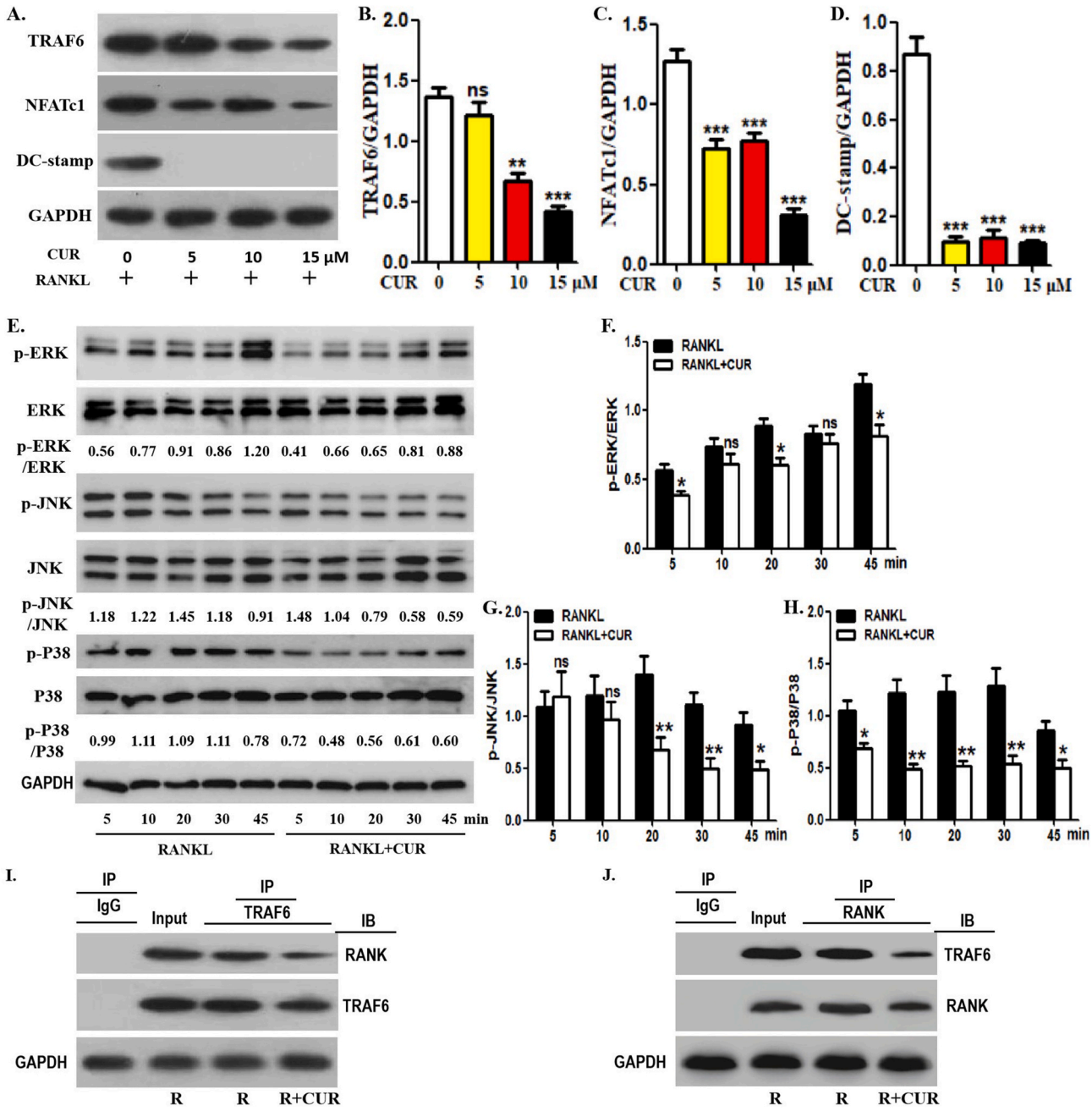

Fig. 2. Curcumin inhibits RANKL-promoted osteoclast-related protein expression in OCPs. (A) After the intervention with different concentration of curcumin (0, 5, 10 or 15 μM), the protein expression levels of TRAF6, NFATc1 and DC-stamp in OCPs were detected using Western-Blot assays. The samples came from the same experiment, and different gels were processed in parallel. (B–D) The histogram displays the relative quantitative results of protein levels in **A**. (E) With RANKL intervention, OCPs were treated with or without curcumin for the indicated times in α-MEM with 1% FBS (appropriate starvation for enhancing the phosphorylation effect). p-ERK, p-JNK and p-P38 were detected using Western-Blot assays. The expression of phosphorylated proteins is represented by the ratio of phosphorylated protein to total protein. The samples came from the same experiment, and different gels were processed in parallel. (F–H) The histogram displays the relative quantitative results of protein levels in **E**. (I–J) The lysates of corresponding OCPs were extracted with anti-TRAF6 or anti-RANK antibody for coimmunoprecipitation, and then the precipitation was detected by Western-Blot analyses with anti-RANK or anti-TRAF6 antibody, respectively. The samples came from the same experiment, and different gels were processed in parallel. The data are expressed as mean ± SEM from three independent experiments. ns, not significant; R, RANKL; CUR, curcumin; IP, the antibody for immunoprecipitation; IB, the antibody for immunoblot.

The tibiae and femurs were taken, wrapped in the gauze soaked in 0.9% saline and stored at −20 °C. All experimental protocols were approved by the Ethics Committee of Fujian Provincial Hospital (2019–0134).

Micro-computed tomography (Micro-CT) analyses

Bruker Micro-CT Skyscan 1276 system (Kontich, Belgium) was used for three-dimensional (3D) analysis of the cancellous bones in the distal femur metaphysis. The scanning settings were as following: voxel size 6.533481 μm, medium resolution, 55 kV, 200 mA, 1 mm Al filter and integration time 384 ms. Bone mineral density measurements were calibrated according to manufacturer's calcium hydroxyapatite (CaHA) model. The analysis was carried out using manufacturer's evaluation software. Three dimensional (3D) reconstruction was completed by NRecon (version 1.7.4.2). The parameters in the area between 2% and 10% proximal to the growth plate consisted of Bone Mineral Density

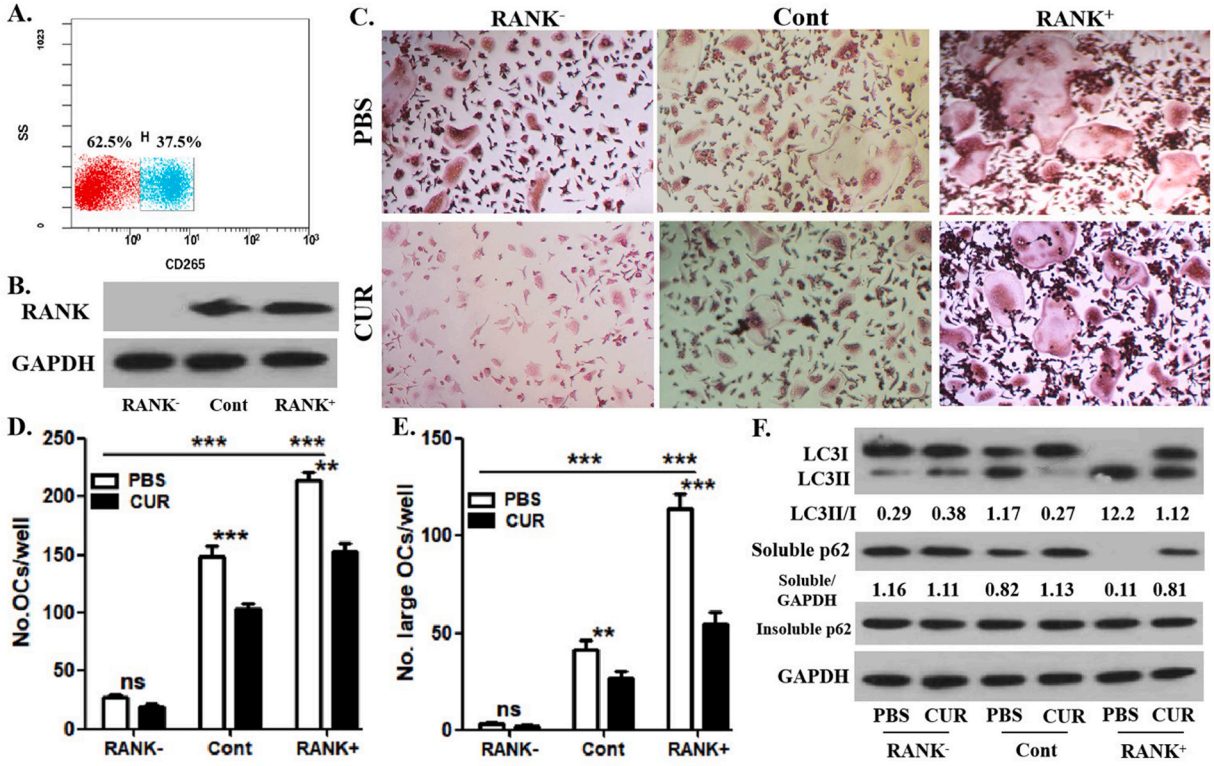

Fig. 3. Curcumin has no effect on the autophagic activity of RANK$^-$ OCPs. (A) The FACS plots related to cell sorting and the percentage of each fraction. (B) After FACS of OCPs induced by RANKL + M-CSF for 1 day, RANK protein expression was detected using Western-Blot assays. (C) The enriched OCPs continued to be induced by RANKL + M-CSF for 3 days with curcumin or PBS, and the formed TRAP$^+$ multinucleate cells in each group are regarded as differentiated osteoclasts. Scale bar, 50 μm. (D) The histogram represents the quantitative results of differentiated osteoclasts in **C**. (E) The histogram represents the quantitative results of large osteoclasts over 5 nuclei in **C**. (F) The enriched OCPs continued to be induced by RANKL for 12 h with curcumin or PBS, and LC3 and p62 protein expression in OCPs were detected using Western-Blot assays. LC3 conversion rate was defined as the ratio of LC3II/LC3I. The samples came from the same experiment, and different gels were processed in parallel. The data are expressed as mean ± SEM from three independent experiments. $^{**}p < 0.01$; $^{***}p < 0.001$. ns, not significant; Cont, control group without sorting; CUR, curcumin.

(BMD), Bone Volume/Tissue Volume (BV/TV), Trabecular Thickness (Tb.Th), Trabecular Number (Tb.N), Bone Surface/Bone Volume (BS/BV), and Trabecular Separation (Tb.Sp) (N = 6, per group). And the area from 20% to 30% proximal to the growth plate was used to measure the thickness of cortical bone, whose parameters consisted of Cortical Bone Volume/Tissue Volume (Ct.BV/TV) and Cortical thickness (Ct.Th).

Haematoxylin and eosin (H&E) and TRAP staining in bone tissues

The indicated tibiae from all mice were fixed in 4% paraformaldehyde (PFA) for 48 h and decalcified in 10% EDTA (pH 7.3) for 2 weeks at 4 °C. Subsequently, all specimens were dehydrated in graded ethanol series and embedded in paraffin. All sections (5 μm thick) were stained with the H&E or TRAP staining kit (N = 6, per group). Image-Pro Plus (IPP, version 7.0) software was used to analyze trabecular bone area (%Tb.Ar) of the H&E-stained sections. The eyepiece grid was used to evaluate the number of osteoclasts in TRAP-stained sections.

Cellular immunofluorescence assays

The isolated RANK$^+$ CSF1R$^+$ OCPs were inoculated on 6-cm dishes and fixed with 4% PFA. After perforation, the cells were blocked with 1% bovine serum albumin (BSA) and incubated with anti-TRAF6 (1:100) antibody (Santa Cruz Biotechnology) overnight at 4 °C. Subsequently, OCPs were stained with fluorochrome-labelled secondary antibody for 30 min, and then counterstained with DAPI for 15 min. Ultimately, the stained cells were visualized and recorded under fluorescence microscope (Olympus IX71, Tokyo, Japan).

Detection of apoptosis

The level of apoptosis was assessed by Annexin V-FITC/PI staining and apoptotic protein detection. After specific treatment based on the experimental design, the indicated cells were collected and stained according to the manufacturer's protocols. Subsequently, the flow cytometer (BD Accuri C6 Plus, BD Biosciences, NJ, USA) was used to measure and quantitatively analyze the level of apoptosis. Apoptotic proteins were detected by Western-Blot assays.

Statistical analyses

All data are expressed as mean ± SEM. Statistical analyses were carried out using one-way or two-way ANOVA. Tukey test was used for Post-Hoc multiple comparisons of one-way or two-way ANOVA. The threshold for the *p*-value is set to 0.05. All statistical analyses were performed using spss19.0 software.

Results

Curcumin inhibited RANKL-promoted OCP autophagy

We first verified the effect of curcumin on the autophagic activity of OCPs under RANKL intervention. Curcumin and RANKL promoted the conversion rate of LC3 (Defined as the ratio of LC3II/LC3I) and the formation of autophagosomes and autolysosomes in OCPs (observed by TEM) [Fig. 1A-D]. However, the ratio of LC3II/LC3I and the number of autophagosomes and autolysosomes in OCPs promoted by RANKL were inhibited by curcumin [Fig. 1A-D]. In addition, both curcumin and

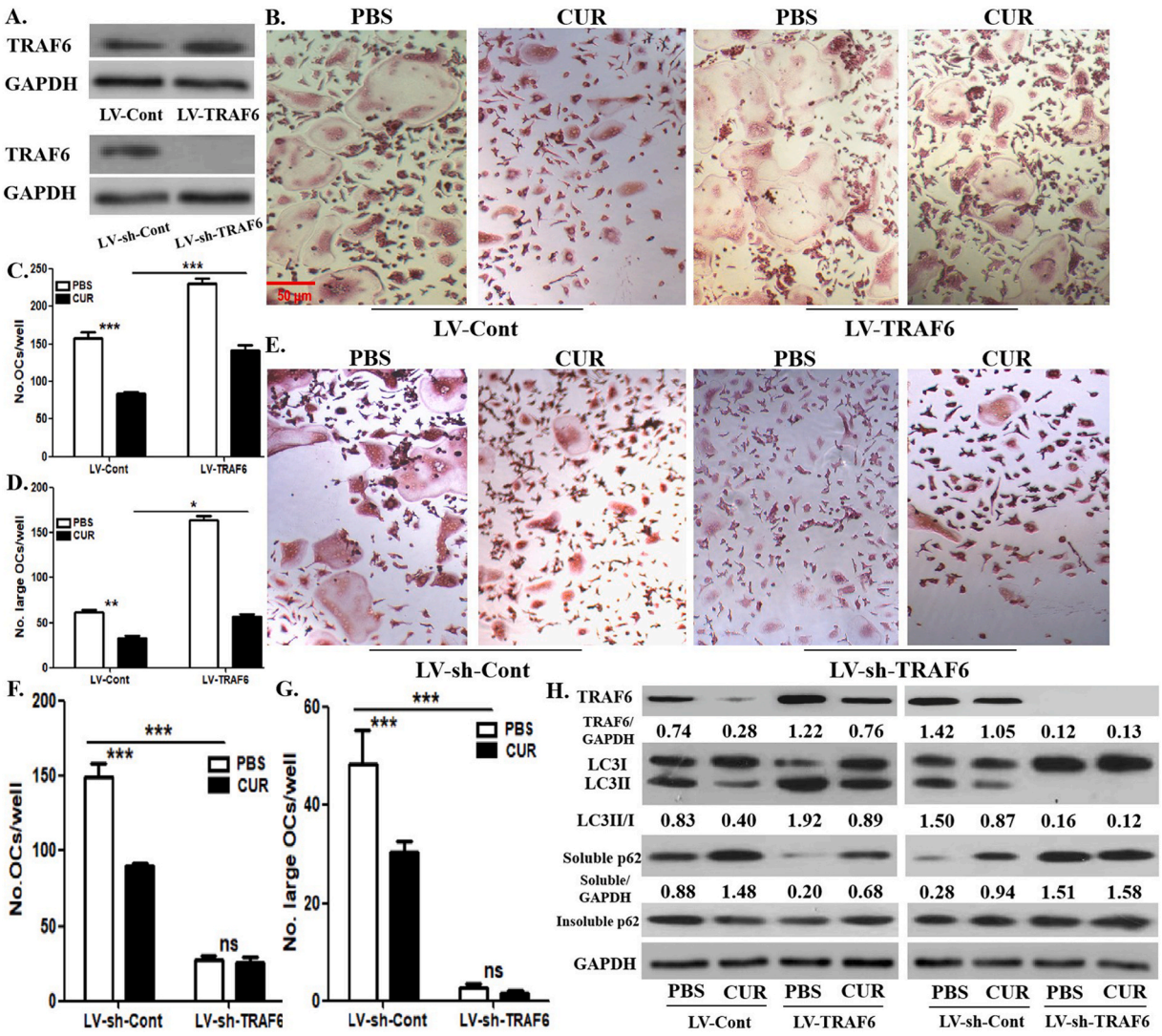

Fig. 4. Curcumin-inhibited autophagy is recovered by TRAF6 overexpression, and curcumin did not affect autophagy under TRAF6 silencing in OCPs. (A) After TRAF6 overexpression or TRAF6 silencing in OCPs treated with RANKL + M-CSF for 1 day, lentiviral transduction efficiency was identified using Western-Blot assays. (B) TRAF6-overexpressed OCPs continued to be induced using RANKL + M-CSF for 3 days with curcumin or PBS, and the formed $TRAP^+$ multinucleate cells in each group are regarded as differentiated osteoclasts. Scale bar, 50 μm. (C) The histogram represents the quantitative results of differentiated osteoclasts in **B**. (D) The histogram represents the quantitative results of large osteoclasts over 5 nuclei in **B**. (E) TRAF6-silenced OCPs continued to be induced using RANKL + M-CSF for 3 days with curcumin or PBS, and the formed $TRAP^+$ multinucleate cells in each group are regarded as differentiated osteoclasts. Scale bar, 50 μm. (F) The histogram represents the quantitative results of differentiated osteoclasts in **E**. (G) The histogram represents the quantitative results of large osteoclasts over 5 nuclei in **E**. (H) TRAF6-overexpressed or TRAF6-silenced OCPs continued to be induced by RANKL for 12 h with curcumin or PBS, and LC3 and p62 protein expression in OCPs were detected using Western-Blot assays. LC3 conversion rate was defined as the ratio of LC3II/LC3I. The samples came from the same experiment, and different gels were processed in parallel. The data are expressed as mean ± SEM from three independent experiments. $^*p < 0.05$; $^{**}p < 0.01$; $^{***}p < 0.001$. ns, not significant; CUR, curcumin.

RANKL inhibited the expression of soluble p62, and curcumin administration partially reversed the effect of RANKL [Fig. 1A]. Nevertheless, insoluble p62 remained stable in all experimental groups [Fig. 1A]. As an autolysosome maturation inhibitor, chloroquine can be used to verify whether the alteration of LC3 conversion is based on the stability of autophagic flux. Furthermore, the addition of chloroquine increased LC3 conversion in all groups. The pattern of increased LC3 conversion in the presence of chloroquine in all groups was similar to that in the absence of chloroquine [Fig. 1B]. These results identified the fluency of autophagic flux. Therefore, the effectiveness of curcumin was verified in this experimental system.

Curcumin repressed signal transduction downstream of RANKL in OCPs

Next, we confirmed the effect of curcumin on the downstream signaling pathway of RANKL by detecting the expression of several osteoclast-related proteins. As shown in [Fig. 2A, B], curcumin inhibited TRAF6 protein expression in OCPs in a concentration-dependent manner in the presence of RANKL. In addition, curcumin significantly inhibited the expression of NFATc1 and DC-stamp from 5 μM [Fig. 2A, C, D]. MAPK signaling molecules in OCPs are activated downstream of RANK/TRAF6 under RANKL induction. Here, changes in the expression of several key proteins related to the MAPK signaling pathway were observed under curcumin intervention. The expression of phosphorylated ERK (p-ERK) decreased significantly except at the 10 and 30 min time points under curcumin intervention [Fig. 2E,F]. The expression of p-JNK was reduced by curcumin, except at 5 and 10 min [Fig. 2E, G]. p-P38 levels were significantly downregulated by curcumin at all time points [Fig. 2E, H]. Therefore, curcumin inhibits the expression of RANKL-related signal transduction molecules in OCPs. Furthermore,

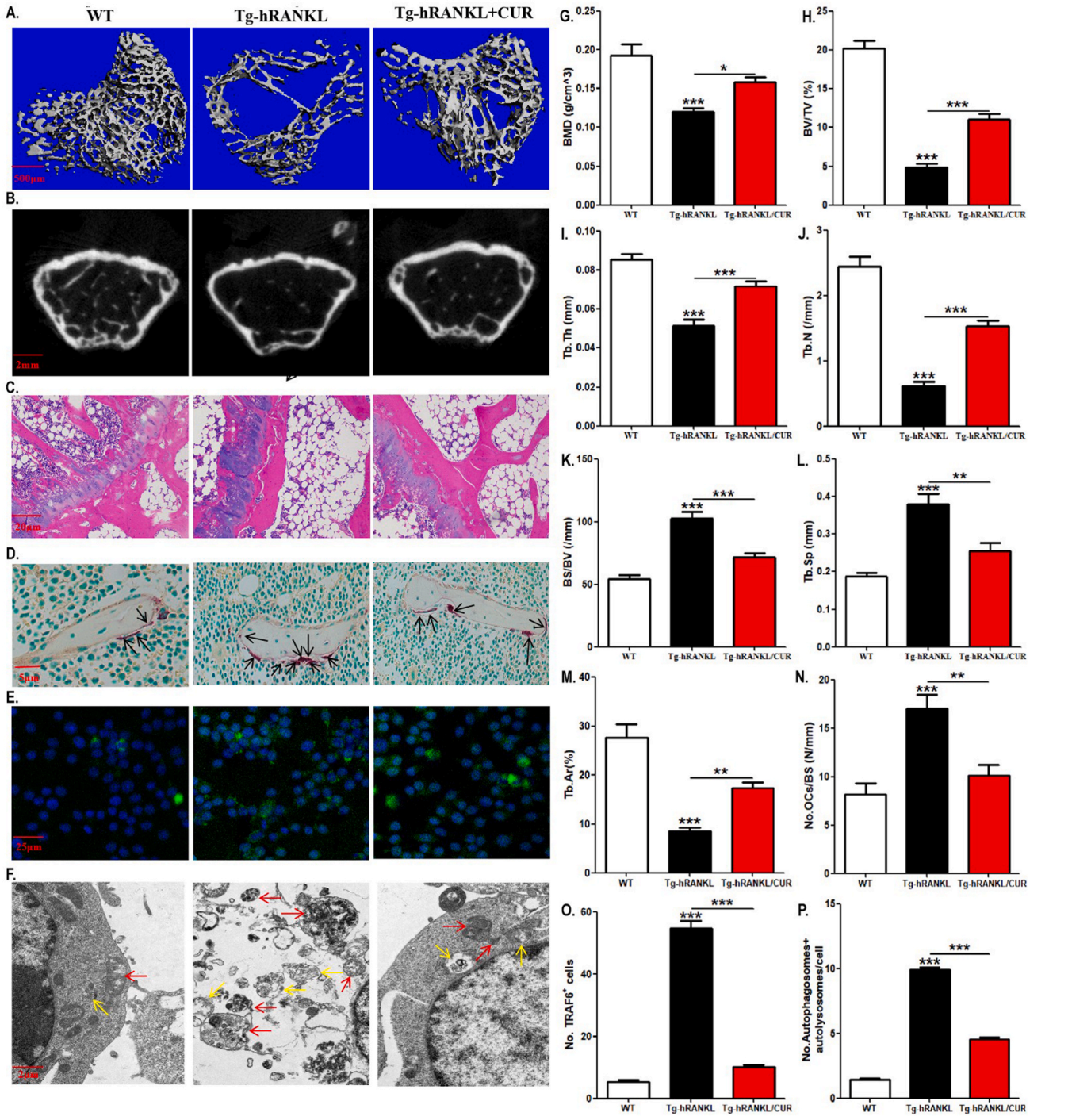

Fig. 5. The enhanced osteoclast formation and OCP autophagy in Tg-hRANKL mice are reversed by curcumin. (A) Representative 3D micro-CT reconstructed images of the femurs from Tg-hRANKL mice fed with 200 mg/kg curcumin or the control diet (for 4 weeks; N = 6–10/group) and control mice in the same nest (WT mice) showing bone mass and bone microstructure (N = 6/group). Scale bar, 2 mm. (B) Representative H&E-stained tibial sections from each group. Scale bar, 20 μm. (C) Representative TRAP-stained tibial sections from each group (Black arrows indicate $TRAP^+$ cells). Scale bar, 5 μm. (D) Representative fluorescent images of TRAF6 in bone marrow $RANK^+$ $CSF1R^+$ cells sorted by FACS. Scale bar, 25 μm. (E) Representative TEM images of autophagosomes (red arrows) and autolysosomes (yellow arrows) in bone marrow $RANK^+$ $CSF1R^+$ cells. Scale bar, 2 μm. (F–L) The trabecular bone parameters, including BMD, BV/TV, BS/BV, Tb.Th, Tb.N, and Tb. Sp, were analysed via micro-CT. (M) The trabecular bone parameter, Tb.Ar, was analysed via H&E staining and IPP system. (N) The number of osteoclasts per millimeter of trabecular bone surface was counted. (O) The percentages of TRAF6-positive cells in **E** (30 cells per field, N = 5). (P) The quantitative results of autophagosomes and autolysosomes in **F** (75 cells from 3 independent experiments). The data are expressed as mean ± SEM. *$p < 0.05$; **$p < 0.01$; ***$p < 0.001$. WT, control mice in the same nest; CUR, curcumin.

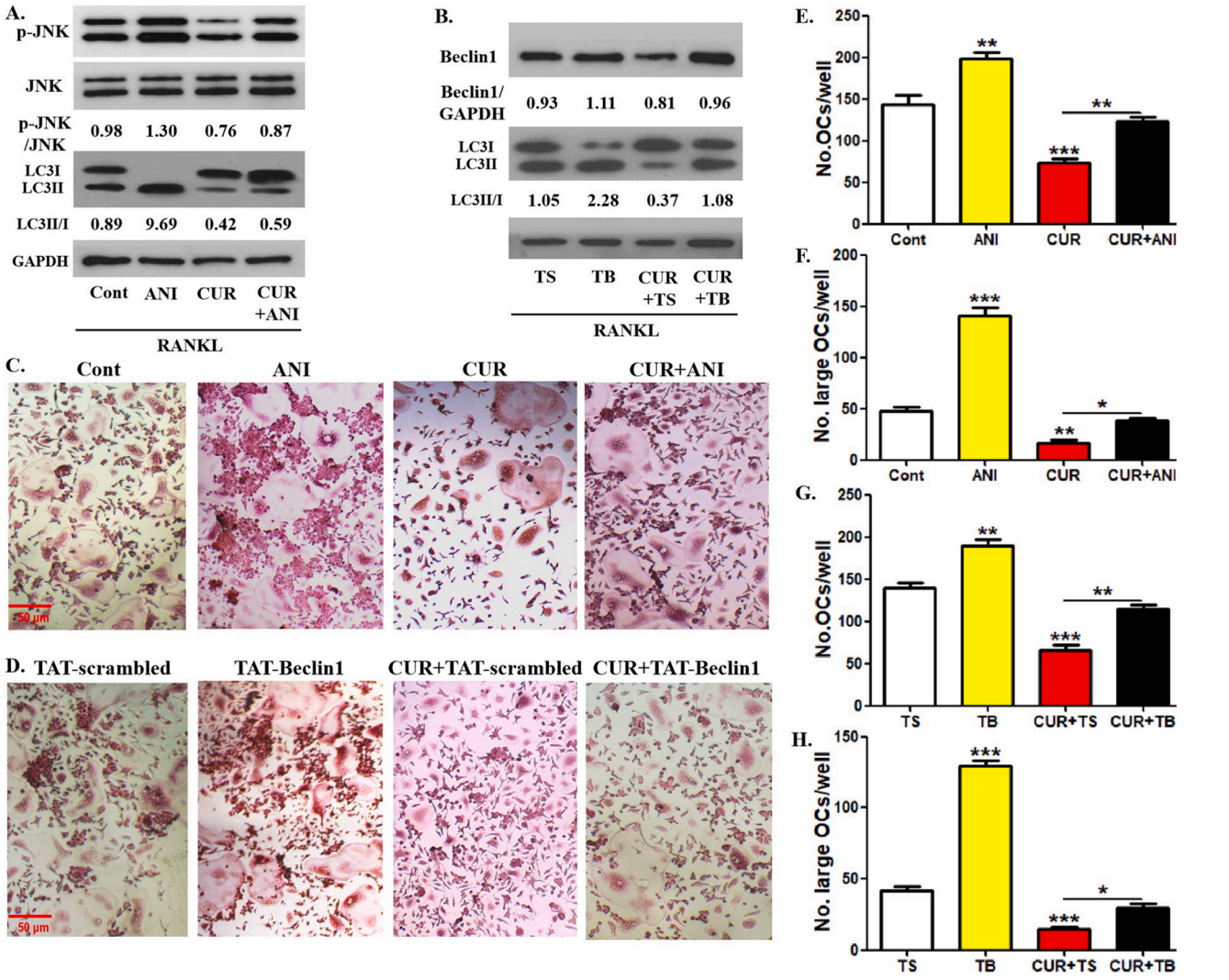

Fig. 6. Curcumin-inhibited OCP autophagy are reversed by anisomycin or TAT-Beclin1. (A) In the presence or absence of anisomycin (5 ng/ml), p-JNK and LC3 protein expression in OCPs treated with curcumin for 8 h were detected using Western-Blot assays. LC3 conversion rate was defined as the ratio of LC3II/LC3I. The samples came from the same experiment, and different gels were processed in parallel. (B) In the presence of TAT-Beclin1 (10 μM) or the control peptide (TAT-scrambled), p-JNK and LC3 protein expression in OCPs treated with curcumin for 8 h were detected using Western-Blot assays. LC3 conversion rate was defined as the ratio of LC3II/LC3I. The samples came from the same experiment, and different gels were processed in parallel. (C) In the presence or absence of anisomycin (5.0 ng/ml), OCPs were induced using RANKL + M-CSF for 4 days with curcumin, and the formed TRAP + multinucleate cells in each group are regarded as differentiated osteoclasts. Scale bar, 50 μm. (D) In the presence of TAT-Beclin1 or TAT-scrambled, OCPs were induced using RANKL + M-CSF for 4 days with curcumin, and the formed TRAP + multinucleate cells in each group are regarded as differentiated osteoclasts. Scale bar, 50 μm. (E) The histogram represents the quantitative results of differentiated osteoclasts in **C**. (F) The histogram represents the quantitative results of large osteoclasts over 5 nuclei in **C**. (G) The histogram represents the quantitative results of differentiated osteoclasts in **D**. (H) The histogram represents the quantitative results of large osteoclasts over 5 nuclei in **D**. The data are expressed as mean ± SEM from three independent experiments. *$p < 0.05$; **$p < 0.01$; ***$p < 0.001$. Cont, control group with PBS; CUR, curcumin; ANI, anisomycin; TS, TAT-scrambled; TB, TAT-Beclin1.

curcumin inhibited the coimmunoprecipitation level of RANK and TRAF6 in OCPs in the presence of RANKL [Fig. 2I, J]. These results suggest that curcumin suppresses signal transduction downstream of RANKL in OCPs.

Curcumin had no effect on the autophagic activity of RANK$^-$ OCPs

To understand the impact of curcumin on OCP autophagy related to RANKL signaling, we sorted OCPs cultured with RANKL + M-CSF for 12 h into RANK$^+$ OCPs (37.5%) and RANK$^-$ OCPs (62.5%) by using fluorescence-activated cell sorting (FACS) [Fig. 3A]. The sorting efficiency was identified through WB analysis [Fig. 3B]. As shown in Fig. 3C-E, RANK$^+$ OCPs had higher osteoclastic differentiation capacity than the control and RANK$^-$ OCPs. The osteoclastic differentiation of RANK$^-$ OCPs was also significantly attenuated [Fig. 3C-E]. The number of differentiated osteoclasts derived from RANK$^+$ and control OCPs was significantly decreased by the application of curcumin [Fig. 3C , D]. However, the number of osteoclasts derived from RANK$^-$ OCPs was not very affected by curcumin administration [Fig. 3C, D]. Furthermore, the number of large osteoclasts (over 5 nuclei) derived from RANK$^+$ and control OCPs was significantly reduced by the addition of curcumin [Fig. 3C, E]. However, the large osteoclasts derived from RANK$^-$ OCPs were not effectively affected by curcumin administration [Fig. 3C, E]. These results elucidated the role of RANK in curcumin-inhibited osteoclast formation and demonstrated the reliability of this experimental system. As shown in [Fig. 3F], curcumin effectively decreased the ratio between LC3II/LC3I and increased the expression of soluble p62 in RANK$^+$ and control OCPs but had no significant effect on the ratio of

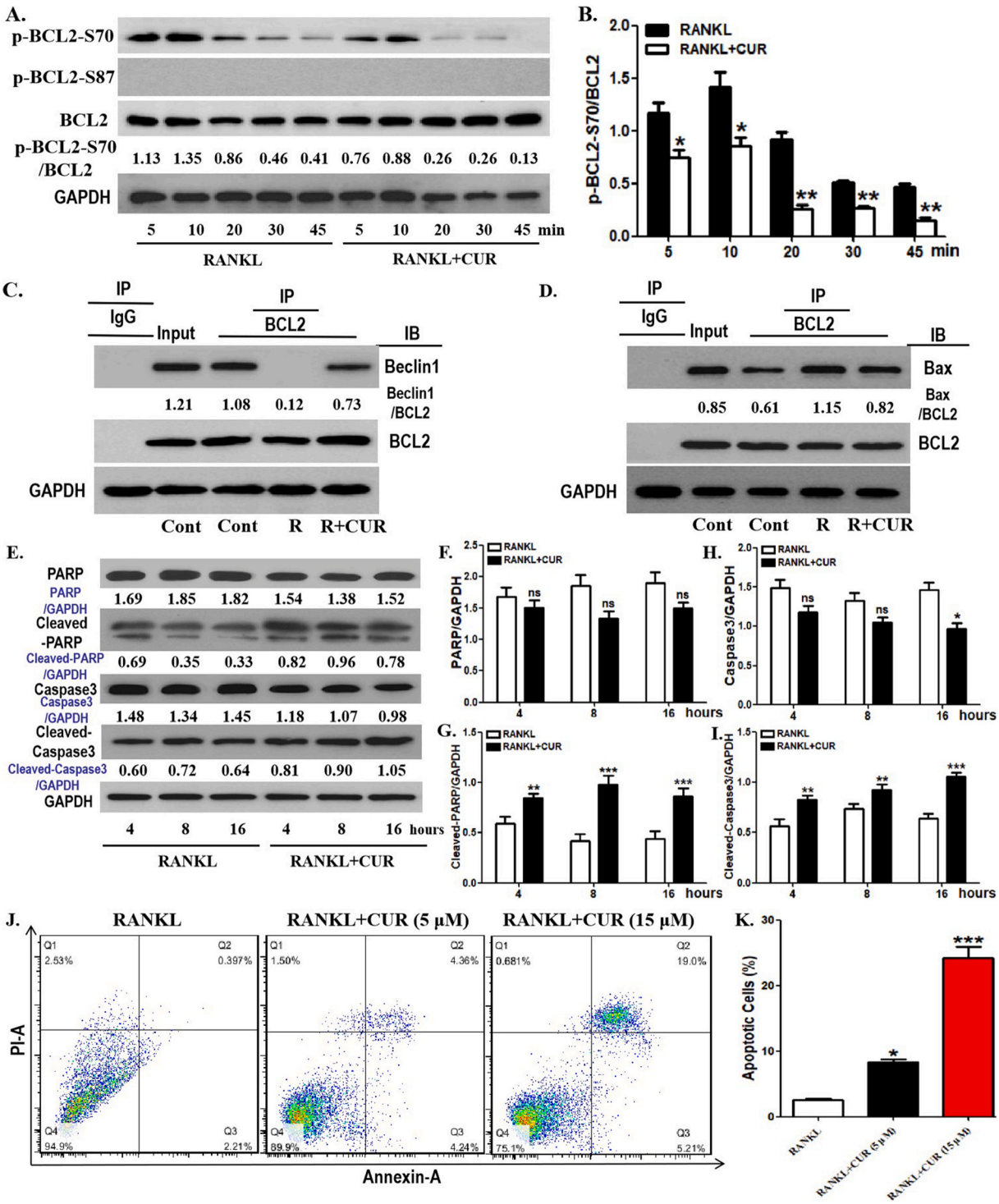

Fig. 7. Curcumin inhibits BCL2 phosphorylation at S70 in OCPs. (A) With RANKL intervention, OCPs were treated with or without curcumin for the indicated times in α-MEM with 1% FBS. p-BCL2-S70 and p-BCL2-S87 protein levels were detected using Western-Blot assays. The expression of phosphorylated proteins is represented by the ratio of phosphorylated protein to total protein. The samples came from the same experiment, and different gels were processed in parallel. (B) The lysates of corresponding OCPs were extracted with anti-BCL2 antibody for coimmunoprecipitation, and then the precipitation was detected by Western-Blot analyses with anti-Beclin1 antibody. The samples came from the same experiment, and different gels were processed in parallel. (C) The lysates of corresponding OCPs were extracted with anti-BCL2 antibody for coimmunoprecipitation, and then the precipitation was detected by Western-Blot analyses with anti-Bax antibody. The samples came from the same experiment, and different gels were processed in parallel. (D) OCPs were treated with or without curcumin for the indicated times in the presence of RANKL. The protein levels of PARP, Cleaved-PARP, Caspase3 and Cleaved-Caspase3 were detected using Western-Blot assays. The samples came from the same experiment, and different gels were processed in parallel. (E, F) The histogram represents the quantitative results of apoptotic protein in **D**. (G) OCPs were treated with RANKL along with corresponding concentrations of curcumin for 48 h. Cell apoptosis was assessed by flow cytometry of Annexin/PI staining. (H) The percentages of apoptotic OCPs (Annexin-A-positive cells) are shown in the histograms according to the results in **G**. The data are expressed as mean ± SEM from three independent experiments. $^{*}p < 0.05$; $^{**}p < 0.01$; $^{***}p < 0.001$. Cont, control group with PBS only; R, RANKL; CUR, curcumin; IP, the antibody for immunoprecipitation; IB, the antibody for immunoblot.

LC3II/LC3I and soluble p62 expression in RANK$^-$ OCPs. In addition, there was no difference in the expression of insoluble p62 between the above groups, which suggested the stability of autophagic flux [Fig. 3F]. Thus, the inhibition of RANKL-promoted OCP autophagy through RANK signaling by curcumin was demonstrated.

Curcumin-inhibited autophagy was recovered by TRAF6 overexpression, and curcumin did not affect autophagy under TRAF6 silencing in OCPs

To further explore the significance of RANKL signaling in curcumin-regulated OCP autophagy, we upregulated and downregulated the TRAF6 gene in OCPs cultured with RANKL + M-CSF for 12 h using a lentiviral transduction technology. The overexpression or silencing efficiency was identified through WB analyses (Fig. 4A). The differentiated osteoclasts derived from control OCPs were significantly reduced by curcumin administration, which was recovered by TRAF6 overexpression [Fig. 4B, C]. In addition, TRAF6 silencing significantly reduced the number of differentiated osteoclasts, but the differentiation of osteoclasts derived from TRAF6-silenced OCPs were not affected by treatment of curcumin [Fig. 4E, F]. Similarly, the large osteoclasts derived from corresponding OCPs exhibited the same trend as mature osteoclasts [Fig. 4B-G]. This clarified the role of TRAF6 in curcumin-regulated osteoclast formation, which indicates the validity of our experimental system. As shown in Fig. 4H], TRAF6 overexpression reversed curcumin-inhibited LC3 conversion and -promoted soluble p62 expression in OCPs. Furthermore, TRAF6 knockdown inhibited the ratio of LC3II/LC3I in OCPs and promoted soluble p62 expression [Fig. 4H]. However, curcumin did not affect the above autophagy parameters of OCPs with TRAF6 knockdown [Fig. 4H]. In addition, there was no difference in the expression of insoluble p62 between the above groups, which suggested the stability of autophagic flux [Fig. 4H]. Overall, the inhibition of RANKL-promoted OCP autophagy through TRAF6 signaling by curcumin was demonstrated.

The enhanced osteoclast formation and OCP autophagy in Tg-hRANKL mice were reversed by curcumin

We documented the role of the signaling pathway downstream of RANKL in curcumin-regulated OCP autophagy *in vitro*. Next, we used Tg-hRANKL mice to observe the *in vivo* effect of RANKL-RANK signaling on curcumin-regulated OCP autophagy. Due to the overexpression of RANKL, Tg-hRANKL mice are a typical animal model of osteoporosis [35,36]. Micro-CT revealed that Tg-hRANKL mice showed obvious bone loss, destroyed bone microstructure, and osteoporotic bone parameters [Fig. 5A a, B, G-L] and [Supplementary Fig. 1A–C]. Compared to WT mice, Tg-hRANKL mice had decreased BMD, BV/TV, Tb.Th, Tb.N, Ct. BV/TV and Ct. Th as well as increased BS/BV and Tb. Sp [Fig. 5G-L]and [Supplementary Fig. 1A–C]. Moreover, H&E staining showed that the bone loss phenotype of Tg-hRANKL mice resulted in thinner growth plates, reduced and disordered trabecular bone, enlarged bone marrow cavity, and increased fat [Fig. 5C]. Quantitative results further showed that Tg-hRANKL mice had an area of decreased trabecular bone [Fig. 5M]. Importantly, TRAP staining showed that Tg-hRANKL mice had more osteoclasts than WT mice [Fig. 5D, N]. Nevertheless, the above indices of Tg-hRANKL mice except Ct. BV/TV and Ct. Th were reversed with curcumin intervention [Fig. 5A–D, G-N]. Therefore, the osteoporotic phenotype of Tg-hRANKL mice was confirmed, which supported the effectiveness of our *in vivo* experimental system.

Next, after enriching RANK$^+$ CSF1R$^+$ bone marrow cells (regarded as OCPs in late differentiation), there was an increase in TRAF6-positive OCPs and the number of autophagosomes and autolysosomes in OCPs in Tg-hRANKL mice blocked by the application of curcumin [Fig. 5E, F, O, P]. The results suggest that RANKL-RANK-TRAF6 signaling has an important impact on curcumin-regulated osteoclastic bone loss *in vivo*.

Curcumin-inhibited OCP autophagy were reversed by treatment of anisomycin or TAT-Beclin1

RANK signaling was responsible for curcumin-regulated OCP autophagy in RANKL-induced osteoclastogenesis. Previous studies have demonstrated that RANKL promotes osteoclastogenesis through JNK-mediated BCL2-Beclin1-autophagy activation signaling [14]. From the above results, we have learned that curcumin could inhibit JNK phosphorylation induced by RANKL. To further explore the role of RANK signaling in the efficacy of curcumin, the relationship between JNK-BCL2-Beclin1 signaling and curcumin-regulated OCP autophagy requires further clarification. We used two positive regulatory agents, JNK activator anisomycin and TAT-Beclin1 overexpressing Beclin1, for rescue assays to achieve our goal [37,38]. As shown in [Fig. 6A], in the presence of RANKL, curcumin decreased p-JNK expression level in OCPs, which was recovered with the application of anisomycin. Moreover, anisomycin administration not only enhanced LC3 conversion but also partially reversed curcumin-reduced LC3 conversion in OCPs [Fig. 6A]. In addition, TAT-Beclin1 administration not only enhanced LC3 conversion but also recovered curcumin-inhibited LC3 conversion in OCPs by increasing Beclin1 protein expression [Fig. 6B]. It is suggested that JNK and its downstream Beclin1 are involved in curcumin-inhibited OCP autophagy under RANKL induction. Additionally, anisomycin administration not only increased the number and size of osteoclasts, but also partially recovered the number and size of osteoclasts decreased by curcumin [Fig. 6C, E, F]. The addition of TAT-Beclin1 also exerted a similar effect as anisomycin [Fig. 6D, G, H]. These results indicated that the roles of JNK and Beclin1 exist in curcumin-inhibited osteoclastic differentiation.

Curcumin inhibited BCL2 phosphorylation at S70 in OCPs

JNK and Beclin1 were related to the pharmacological effect of curcumin on OCP autophagy in the presence of RANKL. We have previously demonstrated that RANKL promotes OCP autophagy and osteoclastogenesis through BCL2 phosphorylation at S70 [39]. Accordingly, in RANKL-induced osteoclastogenesis, the relationship between BCL2 phosphorylation at S70 (p-BCL2-S70) and the efficacy of curcumin on OCP autophagy is also worth further investigation. As shown in [Fig. 7A, B], p-BCL2-S70 levels in OCPs were downregulated by curcumin at all time points. In addition, there was no significant expression of p-BCL2-S87 in OCPs in the presence or absence of curcumin [Fig. 7A]. Therefore, it is indicated that BCL2 phosphorylation at S70 is an essential factor of curcumin-inhibited OCP autophagy with RANKL. Previous studies have shown that BCL2 phosphorylation is associated with autophagy and apoptosis [39,40]. Therefore, we further observed the respective protein interaction between autophagy regulatory molecule Beclin1, pro-apoptotic molecule Bax and BCL2 in OCPs under curcumin intervention. As shown in [Fig. 7C] and [Supplementary Fig. 2A], RANKL inhibited the coimmunoprecipitation level of BCL2 and Beclin1 in OCPs, which was partially recovered by curcumin administration. Moreover, RANKL increased the coimmunoprecipitation level of BCL2 and Bax in OCPs, which was partially blocked by curcumin administration [Fig. 7D] [Supplementary Fig. 2B]. These results suggest that curcumin has the ability to alter the effect of RANKL on the interaction between BCL2 and autophagy regulatory molecule or pro-apoptotic molecule in OCPs.

We documented the role of curcumin in the status of pro-apoptotic molecule in OCPs. Bax, released from the BCL2-Bax complex, can promote apoptotic signal transduction. Therefore, the effect of curcumin on OCP apoptosis also needs to be clarified. As shown in [Fig. 7E, G, I], the addition of curcumin increased the protein expression of Cleaved-PARP and Cleaved-Caspase3 in OCPs at all time points. In addition, the differences in the total levels of caspase3 and PARP in most groups were meaningless, except that the total caspase3 at 16 h in the curcumin group was statistically decreased, but the overall trends were generally

opposite to those of Cleaved-Caspase3 and Cleaved-PARP [Fig. 7E, F, H], which is due to apoptotic signal transduction and verifies the rationality of our experimental system. Furthermore, curcumin increased the number of apoptotic OCPs in a concentration-dependent manner [Fig. 7J, K]. These results demonstrated the promoting effect of curcumin on OCP apoptosis.

Discussion

Curcumin, a plant-derived natural compound, can function as a treatment option for osteoporosis, which is characterized by enhanced osteoclast formation, because of curcumin's blocking effect on RANKL-promoted OCP autophagy [11]. As the core osteoclastogenic inducer, RANKL can stimulate a series of downstream cascade reactions by binding to its receptor RANK [23–29]. The activation of OCP autophagy by RANKL is also mediated by RANKL signaling [14,30,31]. In a previous study, we demonstrated that RANKL regulates OCP autophagy through downstream JNK1 signaling [14]. Further exploration of the relationship between curcumin-regulated OCP autophagy and RANKL signaling is conducive to better understanding the role of curcumin in regulating RANKL-induced osteoclast formation and its potential mechanism. Using various biological methods, we were the first to elucidate the significance of RANKL-RANK-TRAF6 signal transduction in curcumin-regulated OCP autophagy and osteoclast formation at the molecular, cellular, and animal levels.

Firstly, we elucidated the direct promoting effect of curcumin on OCP autophagy and its inhibition on RANKL-induced OCP autophagy, which was consistent with the previous results, and identified the reliability of the subsequent experimental data [11]. Curcumin-inhibited signaling molecule expression and signal transduction downstream of RANKL suggest that RANKL-related signaling pathway is involved in curcumin-regulated osteoclast formation. Importantly, after RANK positive-sorting, curcumin decreased the autophagic activity of OCPs, and the number and size of osteoclasts. Nevertheless, curcumin had no effects on the autophagic activity of OCPs, and the number or size of osteoclasts following RANK negative-sorting. In response to RANKL, RANK activates the downstream cascade reaction via TRAF6 signaling, which ultimately leads to osteoclast formation [41,42]. RANKL-promoted OCP autophagy is also mediated by its downstream signaling [14]. Our data confirmed the pivotal value of RANK in curcumin-regulated OCP autophagy and osteoclast formation. Consistent with this, TRAF6 knockdown by RNA interference (RNAi) also caused curcumin to lose its inhibitory effect on OCP autophagy and osteoclast formation. In contrast, TRAF6 overexpression rescued the inhibitory effects of curcumin on OCP autophagy and osteoclast formation. These eresults demonstrated that RANK-TRAF6, a core signaling pathway downstream of RANKL, substantially contributes to curcumin-regulated OCP autophagy and osteoclast formation. *In vivo* experiments revealed that curcumin ameliorated bone loss and excessive osteoclastic activity in transgenic mice overexpressing RANKL. Previous studies showed that there are two states of OCPs *in vivo*: early $RANK^{-}$ OCPs and late $RANK^{+}$ OCPs [43–45]. In order to observe the relationship between curcumin and OCP autophagy related to RANKL signaling, we sorted $RANK^{+}$ $CSF1R^{+}$ bone marrow cells using FACS technique. The results clarified that curcumin suppressed the autophagic response and TRAF6 fluorescent expression in $RANK^{+}$ OCPs of RANKL-overexpressed mice, which is the effective supplements to the above results *in vitro*, and further confirmed that the RANK-TRAF6 signaling participates in curcumin-regulated OCP autophagy.

To extend the significance of RANK signaling in curcumin's efficacy in OCP autophagy, we need to understand the relationship between the intrinsic mechanism underlying RANK-TRAF6 signal transduction and curcumin-regulated OCP autophagy. Previous literatures showed that JNK is the downstream molecule of TRAF6 and phosphorylated by RANKL during osteoclastogenesis [4,27,46,47]. As a positive regulator of autophagy, JNK can enhance the autophagic activity of various histocytes [48–50]. The classic case of JNK-regulated autophagy indicated that under starvation stress, activated JNK can promote the release of Beclin1 from the BCL2-Beclin1 complex, and free Beclin1 enters the autophagic flux to activate autophagy [51]. Our previous study demonstrated that RANKL also stimulates JNK-BCL2-Beclin1 signaling pathway in OCPs, thereby inducing OCP autophagy and osteoclastogenesis [14]. Our experimental data elucidated that curcumin could inhibit JNK phosphorylation in OCPs, and JNK phosphorylation, LC3 transformation and osteoclastogenesis inhibited by curcumin were reversed by JNK pharmacological activation. Combined with previous literatures, our results clarified the role of JNK signaling in curcumin-inhibited OCP autophagy and osteoclastogenesis. Moreover, the pharmacological overexpression of Beclin1 could also recover the inhibitory effect of curcumin on LC3 transformation and osteoclastogenesis. Previous studies have shown that TRAF6 activates autophagy by regulating the autophagy protein Beclin1, which is essential for RANKL-induced osteoclastogenesis [32]. Additionally, TRAF6 overexpression activates JNK phosphorylation in osteoclasts, while silencing TRAF6 attenuates RANKL-induced JNK phosphorylation in OCPs [52,53]. These findings indicate that RANKL-controlled TRAF6 signaling enhances OCP autophagy through Beclin1 or JNK phosphorylation. Therefore, the alterations in the TRAF6-JNK-autophagy activation signaling pathway are supposed to be involved in the inhibitory effect of curcumin on RANKL-induced OCP autophagy, which clarifies the mechanism of the significant role that TRAF6 plays in curcumin's efficacy in OCP autophagy with RANKL. Accordingly, we can infer that curcumin prevents Beclin1-related autophagy by inhibiting JNK signaling downstream of RANK/TRAF6, thereby suppressing RANKL-induced OCP autophagy and osteoclastogenesis.

Next, we also need to confirm the significance of BCL2 phosphorylation governing Beclin1-dependent autophagy for curcumin's efficacy, in order to expound the role of BCL2-Beclin1 signaling in curcumin-regulated OCP autophagy. Our team previously described that RANKL promotes the dissociation of Beclin1 from the BCL2-Beclin1 complex and induces OCP autophagy, in which BCL2 phosphorylation at S70 plays a mediating role [39]. Thus, the value of BCL2 phosphorylation at corresponding sites in curcumin's efficacy also requires clarification. The experimental data showed that curcumin inhibited RANKL-caused BCL2 phosphorylation at S70 but did not affect BCL2 phosphorylation at S87. Furthermore, the protein interaction between BCL2 and Beclin1 inhibited by RANKL in OCPs was partially reversed by the addition of curcumin. Therefore, we further learned that curcumin prevents Beclin1 from entering autophagic flux by inhibiting BCL2 phosphorylation at S70, which determines the inhibitory effect of curcumin on OCP autophagy. In addition, previous study has demonstrated that BCL2 phosphorylation bridges JNK activation and Beclin1-dependent autophagy [51]. We have also elucidated the significance of BCL2 phosphorylation at S70 for JNK-mediated BCL2-Beclin1 complex in OCPs [14]. Combined with previous studies and the above results, we confirmed that due to the inhibition of BCL2 phosphorylation at S70, curcumin affected OCP autophagy and subsequent osteoclastogenesis by preventing JNK-BCL2-Beclin1 signal transduction. In addition, we observed that curcumin could expand OCP apoptosis under RANKL intervention, which is consistent with previous results [54]. Autophagy is known to have an anti-apoptotic effect, especially OCPs in RANKL-induced osteoclastogenesis [14,55–57].

Curcumin can cause opposite alterations in autophagy and apoptosis in various cells. Curcumin mediates mTOR inhibition and BCL2 upregulation by activating AMPK-JNK signaling, thereby enhancing autophagy and inhibiting apoptosis in neurons, respectively, eventually ameliorating cognitive impairment related to neuronal defects caused by cisplatin [58]. Curcumin can also promote the autophagic activity of cardiomyocytes, which prevents cardiomyocytes from undergoing apoptosis [22]. Additionally, Curcumin can reduce the apoptosis of neurons by enhancing autophagy, thus playing a therapeutic role in spinal cord injury in rat [59]. Similar reports also appeared in other

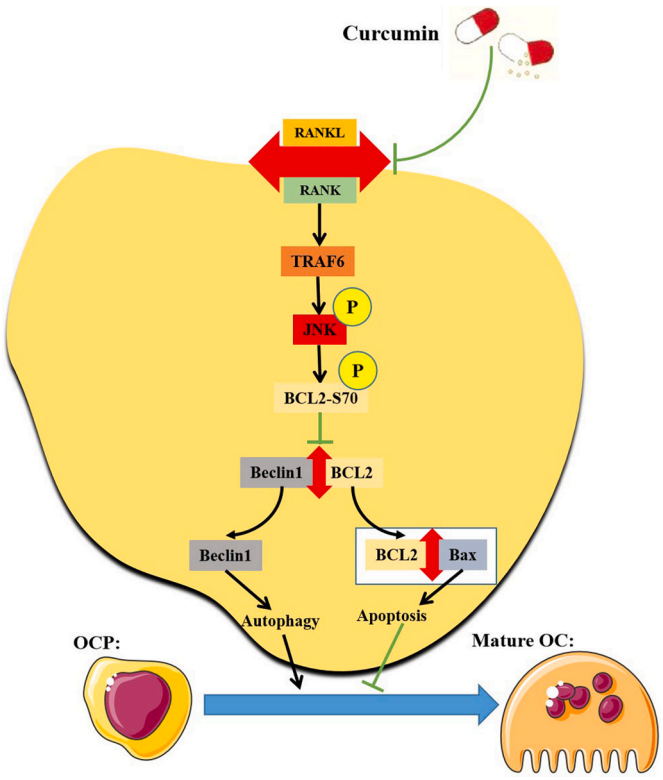

Fig. 8. The Working model diagram of this study. In brief, RANKL binds to its receptor RANK, and then activates the autophagy of OCPs through downstream TRAF6 signaling. The signal transduction downstream of TRAF6 is as follows: after phosphorylation by upstream signaling molecules, activated JNK leads to BCL2 phosphorylation at S70, thereby causing Beclin1 to dissociate from the BCL2-Beclin1 complex, which leads to Beclin1-dependent autophagy, and the differentiation of OCPs into mature osteoclasts. Furthermore, free BCL2 from the BCL2-Beclin1 complex binds to Bax, thereby inhibiting Bax-dependent apoptosis, which is also a promoter of osteoclast differentiation. Curcumin can inhibit the formation of mature osteoclasts by inhibiting RANKL-RANK-TRAF6-JNK-BCL2-Beclin1-autophagy activation signal transduction.

studies [60–62]. Our data indicated that curcumin simultaneously inhibits RANKL-promoted OCP autophagy and promotes RANKL-related OCP apoptosis, suggesting that there also exists a regulatory relationship between autophagy and apoptosis in OCPs under curcumin intervention. Moreover, previous studies reported that BCL2 phosphorylation at S70 exerts an anti-apoptotic function [63,64]. In a previous study, we highlighted that the anti-apoptotic effect of BCL2 phosphorylation at S70 is based on autophagy activation [39]. In this study, the RANKL-enhanced protein interaction between BCL2 and Bax in OCPs was partially blocked by the addition of curcumin. Alterations in the interaction between BCL2 and Beclin1 affect the binding of BCL2 and Bax, which is based on free BCL2 molecules [39,65]. Thus, we believe that with the induction of RANKL, curcumin decreases BCL2 binding to Bax by promoting the interaction of BCL2 and Beclin1 in OCPs, which enhances Bax-dependent apoptotic signal transduction. These results support the regulatory effect of curcumin-inhibited autophagy on curcumin-promoted apoptosis during RANKL-induced osteoclastogenesis. Furthermore, curcumin-promoted OCP apoptosis is also explained to a certain extent from the perspective of protein interactions based on autophagy regulatory molecules. Our current working model is shown in [Fig. 8].

Conclusion

Curcumin has been shown to suppress RANKL-induced OCP autophagy and osteoclast formation [10–13]. Our results build on those of previous studies by demonstrating the significance of signal transduction downstream of RANKL in the therapeutic effect of curcumin. Therefore, our study not only reveals the potential mechanism underlying curcumin-inhibited osteoclast formation, namely the RANK-TRAF6-JNK-BCL2-Beclin1-autophagy signaling pathway, but also provides more evidence for optimizing the application of curcumin in the treatment of osteoclastic osteoporosis.

Conflicts of interest

The authors declare that there is no conflict of interests.

Acknowledgments

This work was supported by The Sailing Fund from Fujian Medical University (2018QH1134), Fujian Provincial Natural Science Foundation Projects (2020J011079), The Postdoctoral Science Foundation of China (2022M710702), Major scientific research project of health in Fujian Province (20212D01003), and Special subsidy for scientific research of Fujian Provincial Department of Finance (20213964).

Appendix A. Supplementary data

Supplementary data to this article can be found online at https://doi.org/10.1016/j.bj.2023.100605.

References

[1] Yu W, Zhong L, Yao L, Wei Y, Gui T, Li Z, et al. Bone marrow adipogenic lineage precursors promote osteoclastogenesis in bone remodeling and pathologic bone loss. J Clin Invest 2021;131(2):e140214.
[2] Fujii T, Murata K, Mun SH, Bae S, Lee YJ, Pannellini T, et al. MEF2C regulates osteoclastogenesis and pathologic bone resorption via c-FOS. Bone Res 2021;9(1):4.
[3] Yang W, Lu X, Zhang T, Han W, Li J, He W, et al. TAZ inhibits osteoclastogenesis by attenuating TAK1/NF-κB signaling. Bone Res 2021;9(1):33.
[4] Boyle WJ, Simonet WS, Lacey DL. Osteoclast differentiation and activation. Nature 2003;423(6937). 337-42.
[5] Xiong J, Cawley K, Piemontese M, Fujiwara Y, Zhao H, Goellner JJ, et al. Soluble RANKL contributes to osteoclast formation in adult mice but not ovariectomy-induced bone loss. Nat Commun 2018;9(1):2909.
[6] French DL, Muir JM, Webber CE. The ovariectomized, mature rat model of postmenopausal osteoporosis: an assessment of the bone sparing effects of curcumin. Phytomedicine 2008;15(12). 1069-78.
[7] Hussan F, Ibraheem NG, Kamarudin TA, Shuid AN, Soelaiman IN, Othman F. Curcumin protects against ovariectomy-induced bone changes in rat model. Evid Based Complement Alternat Med 2012;2012:174916.
[8] Deng J, Golub LM, Lee HM, Raja V, Johnson F, Kucine A, et al. A novel modified-curcumin promotes resolvin-like activity and reduces bone loss in diabetes-induced experimental periodontitis. J Inflamm Res 2021;14. 5337-47.
[9] Jiang Q, Lei YH, Krishnadath DC, Zhu BY, Zhou XW. Curcumin regulates EZH2/Wnt/β-Catenin pathway in the mandible and femur of ovariectomized osteoporosis rats. Kaohsiung J Med Sci 2021;37(6). 513-9.
[10] Liang Z, Xue Y, Wang T, Xie Q, Lin J, Wang Y. Curcumin inhibits the migration of osteoclast precursors and osteoclastogenesis by repressing CCL3 production. BMC Complement Med Ther 2020;20(1):234.
[11] Ke D, Wang Y, Yu Y, Wang Y, Zheng W, Fu X, et al. Curcumin-activated autophagy plays a negative role in its anti-osteoclastogenic effect. Mol Cell Endocrinol 2020;500:110637.
[12] Von Metzler I, Krebbel H, Kuckelkorn U, Heider U, Jakob C, Kaiser M, et al. Curcumin diminishes human osteoclastogenesis by inhibition of the signalosome-associated I kappaB kinase. J Cancer Res Clin Oncol 2009;135(2). 173-9.
[13] Bharti AC, Takada Y, Aggarwal BB. Curcumin (diferuloylmethane) inhibits receptor activator of NF-kappa B ligand-induced NF-kappa B activation in osteoclast precursors and suppresses osteoclastogenesis. J Immunol 2004;172(10). 5940-7.
[14] Ke D, Ji L, Wang Y, Fu X, Chen J, Wang F, et al. JNK1 regulates RANKL-induced osteoclastogenesis via activation of a novel Bcl-2-Beclin1-autophagy pathway. Faseb J 2019;33(10). 11082-95.
[15] Cheng L, Zhu Y, Ke D, Xie D. Oestrogen-activated autophagy has a negative effect on the anti-osteoclastogenic function of oestrogen. Cell Prolif 2020;53(4):e12789.
[16] DeSelm CJ, Miller BC, Zou W, Beatty WL, van Meel E, Takahata Y, et al. Autophagy proteins regulate the secretory component of osteoclastic bone resorption. Dev Cell 2011;21(5). 966-74.
[17] Lin NY, Chen CW, Kagwiria R, Liang R, Beyer C, Distler A, et al. Inactivation of autophagy ameliorates glucocorticoid-induced and ovariectomy-induced bone loss. Ann Rheum Dis 2016;75(6). 1203-10.

[18] Deng J, Ouyang P, Li W, Zhong L, Gu C, Shen L, et al. Curcumin alleviates the senescence of canine bone marrow mesenchymal stem cells during in vitro expansion by activating the autophagy pathway. Int J Mol Sci 2021;22(21):11356.
[19] Hu P, Ke C, Guo X, Ren P, Tong Y, Luo S, et al. Both glypican-3/Wnt/β-catenin signaling pathway and autophagy contributed to the inhibitory effect of curcumin on hepatocellular carcinoma. Dig Liver Dis 2019;51(1). 120-6.
[20] Zhou T, Ye L, Bai Y, Sun A, Cox B, Liu D, et al. Autophagy and apoptosis in hepatocellular carcinoma induced by EF25-(GSH)2: a novel curcumin analog. PLoS One 2014;9(9):e107876.
[21] Zhang L, Xu S, Cheng X, Wu J, Wu L, Wang Y, et al. Curcumin induces autophagic cell death in human thyroid cancer cells. Toxicol Vitro 2022;78:105254.
[22] Gu Y, Xia H, Chen X, Li J. Curcumin nanoparticles attenuate lipotoxic injury in cardiomyocytes through autophagy and endoplasmic reticulum stress signaling pathways. Front Pharmacol 2021;12:571482.
[23] Lin S, Zhao XL, Wang Z. TANK-binding kinase 1 mediates osteoclast differentiation by regulating NF-κB, MAPK and Akt signaling pathways. Immunol Cell Biol 2021; 99(2). 223-33.
[24] Kim B, Lee KY, Park B. Icariin abrogates osteoclast formation through the regulation of the RANKL-mediated TRAF6/NF-κB/ERK signaling pathway in Raw264.7 cells. Phytomedicine 2018;51. 181-90.
[25] Kobayashi N, Kadono Y, Naito A, Matsumoto K, Yamamoto T, Tanaka S, et al. Segregation of TRAF6-mediated signaling pathways clarifies its role in osteoclastogenesis. EMBO J 2021;20(6). 1271-80.
[26] Armstrong AP, Tometsko ME, Glaccum M, Sutherland CL, Cosman D, Dougall WC. RANK/TRAF6-dependent signal transduction pathway is essential for osteoclast cytoskeletal organization and resorptive function. J Biol Chem 2002;277(46). 44347-56.
[27] David JP, Sabapathy K, Hoffmann O, Idarraga MH, Wagner EF. JNK1 modulates osteoclastogenesis through both c-Jun phosphorylation-dependent and -independent mechanisms. J Cell Sci 2002;115. 4317-25.
[28] Karin M, Cao Y, Greten FR, Li ZW. NF-kappaB in cancer: from innocent bystander to major culprit. Nat Rev Cancer 2002;2(4). 301-10.
[29] Maruyama T, Fukushima H, Nakao K, Shin M, Yasuda H, Weih F, et al. Processing of the NF-kappa B2 precursor p100 to p52 is critical for RANKL-induced osteoclast differentiation. J Bone Miner Res 2010;25(5). 1058-67.
[30] Xiu Y, Xu H, Zhao C, Li J, Morita Y, Yao Z, et al. Chloroquine reduces osteoclastogenesis in murine osteoporosis by preventing TRAF3 degradation. J Clin Invest 2014;124(1):297–310.
[31] Lin NY, Beyer C, Giessl A, Kireva T, Scholtysek C, Uderhardt S, et al. Autophagy regulates TNFα-mediated joint destruction in experimental arthritis. Ann Rheum Dis 2013;72(5). 761-8.
[32] Arai A, Kim S, Goldshteyn V, Kim T, Park NH, Wang CY, et al. Beclin1 modulates bone homeostasis by regulating osteoclast and chondrocyte differentiation. J Bone Miner Res 2019;34(9). 1753-66.
[33] Ha J, Choi HS, Lee Y, Kwon HJ, Song YW, Kim HH. CXC chemokine ligand 2 induced by receptor activator of NF-kappa B ligand enhances osteoclastogenesis. J Immunol 2010;184(9). 4717-24.
[34] Zhi X, Wang L, Chen H, Fang C, Cui J, Hu Y, et al. l-tetrahydropalmatine suppresses osteoclastogenesis in vivo and in vitro via blocking RANK-TRAF6 interactions and inhibiting NF-κB and MAPK pathways. J Cell Mol Med 2020;24(1). 785-98.
[35] Bonnet N, Bourgoin L, Biver E, Douni E, Ferrari S. RANKL inhibition improves muscle strength and insulin sensitivity and restores bone mass. J Clin Invest 2019; 129(8). 3214-23.
[36] Rinotas V, Niti A, Dacquin R, Bonnet N, Stolina M, Han CY, et al. Novel genetic models of osteoporosis by overexpression of human RANKL in transgenic mice. J Bone Miner Res 2014;29(5). 1158-69.
[37] Hazzalin CA, Le Panse R, Cano E, Mahadevan LC. Anisomycin selectively desensitizes signalling components involved in stress kinase activation and fos and jun induction. Mol Cell Biol 1998;18(4). 1844-54.
[38] Atwood DJ, Pokhrel D, Brown CN, Holditch SJ, Bachu DM, Thorburn A, et al. Increased mTOR and suppressed autophagic flux in the heart of a hypomorphic Pkd1 mouse model of autosomal dominant polycystic kidney disease. Cell Signal 2020;74:109730.
[39] Ke D, Yu Y, Li C, Han J, Xu J. Phosphorylation of BCL2 at the Ser70 site mediates RANKL-induced osteoclast precursor autophagy and osteoclastogenesis. Mol Med 2022;28(1):22.
[40] Wei Y, Sinha S, Levine B. Dual role of JNK1-mediated phosphorylation of Bcl-2 in autophagy and apoptosis regulation. Autophagy 2008;4(7). 949-51.
[41] Chen H, Fang C, Zhi X, Song S, Gu Y, Chen X, et al. Neobavaisoflavone inhibits osteoclastogenesis through blocking RANKL signalling-mediated TRAF6 and c-Src recruitment and NF-κB, MAPK and Akt pathways. J Cell Mol Med 2020;24(16). 9067-84.
[42] Chen K, Yan Z, Wang Y, Yang Y, Cai M, Huang C, et al. Shikonin mitigates ovariectomy-induced bone loss and RANKL-induced osteoclastogenesis via TRAF6-mediated signaling pathways. Biomed Pharmacother 2020;126:110067.
[43] Charles JF, Hsu LY, Niemi EC, Weiss A, Aliprantis AO, Nakamura MC. Inflammatory arthritis increases mouse osteoclast precursors with myeloid suppressor function. J Clin Invest 2012;122(12). 4592-605.
[44] Muto A, Mizoguchi T, Udagawa N, Ito S, Kawahara I, Abiko Y, et al. Lineage-committed osteoclast precursors circulate in blood and settle down into bone. J Bone Miner Res 2011;26(12). 2978-90.
[45] Arai F, Miyamoto T, Ohneda O, Inada T, Sudo T, Brasel K, et al. Commitment and differentiation of osteoclast precursor cells by the sequential expression of c-Fms and receptor activator of nuclear factor kappaB (RANK) receptors. J Exp Med 1999; 190(12). 1741-54.
[46] Teitelbaum SL. Bone resorption by osteoclasts. Science 2000;289(5484). 1504-8.
[47] Ikeda F, Nishimura R, Matsubara T, Tanaka S, Inoue J, Reddy SV, et al. Critical roles of c-Jun signaling in regulation of NFAT family and RANKL-regulated osteoclast differentiation. J Clin Invest 2004;114(4). 475-84.
[48] Liu S, Lin H, Wang D, Li Q, Luo H, Li G, et al. PCDH17 increases the sensitivity of colorectal cancer to 5-fluorouracil treatment by inducing apoptosis and autophagic cell death. Signal Transduct Targeted Ther 2019;4:53.
[49] Chen X, Hu Y, Zhang W, Chen K, Hu J, Li X, et al. Cisplatin induces autophagy to enhance hepatitis B virus replication via activation of ROS/JNK and inhibition of the Akt/mTOR pathway. Free Radic Biol Med 2019;131. 225-36.
[50] Cho YL, Tan HWS, Saquib Q, Ren Y, Ahmad J, Wahab R, et al. Dual role of oxidative stress-JNK activation in autophagy and apoptosis induced by nickel oxide nanoparticles in human cancer cells. Free Radic Biol Med 2020;153. 173-86.
[51] Wei Y, Pattingre S, Sinha S, Bassik M, Levine B. JNK1-mediated phosphorylation of Bcl-2 regulates starvation-induced autophagy. Mol Cell 2008;30(6). 678-88.
[52] Ikeda F, Matsubara T, Tsurukai T, Hata K, Nishimura R, Yoneda T. JNK/c-Jun signaling mediates an anti-apoptotic effect of RANKL in osteoclasts. J Bone Miner Res 2008;23(6). 907-14.
[53] Choi JH, Jang AR, Park MJ, Kim DI, Park JH. Melatonin inhibits osteoclastogenesis and bone loss in ovariectomized mice by regulating PRMT1-mediated signaling. Endocrinology 2021;162(6):bqab057.
[54] Ozaki K, Kawata Y, Amano S, Hanazawa S. Stimulatory effect of curcumin on osteoclast apoptosis. Biochem Pharmacol 2000;59(12). 1577-81.
[55] Wang J, Zhou X, Wang H, Xiao Q, Ding K, Dong X, et al. Autophagy-inhibiting polymer as an effective nonviral cancer gene therapy vector with inherent apoptosis-sensitizing ability. Biomaterials 2020;255:120156.
[56] Young TM, Reyes C, Pasnikowski E, Castanaro C, Wong C, Decker CE, et al. Autophagy protects tumors from T cell-mediated cytotoxicity via inhibition of TNFα-induced apoptosis. Sci Immunol 2020;5(54):eabb9561.
[57] Ke D, Zhu Y, Zheng W, Fu X, Chen J, Han J. Autophagy mediated by JNK1 resists apoptosis through TRAF3 degradation in osteoclastogenesis. Biochimie 2019;167. 217-7.
[58] Yi LT, Dong SQ, Wang SS, Chen M, Li CF, Geng D, et al. Curcumin attenuates cognitive impairment by enhancing autophagy in chemotherapy. Neurobiol Dis 2020;136:104715.
[59] Li W, Yao S, Li H, Meng Z, Sun X. Curcumin promotes functional recovery and inhibits neuronal apoptosis after spinal cord injury through the modulation of autophagy. J Spinal Cord Med 2021;44(1):37–45.
[60] Lan T, Guo H, Lu X, Geng K, Wu L, Luo Y, et al. Dual-responsive curcumin-loaded nanoparticles for the treatment of cisplatin-induced acute kidney injury. Biomacromolecules 2022;23(12). 5253-66.
[61] Yao Q, Ke ZQ, Guo S, Yang XS, Zhang FX, Liu XF, et al. Curcumin protects against diabetic cardiomyopathy by promoting autophagy and alleviating apoptosis. J Mol Cell Cardiol 2018;124:26–34.
[62] Li X, Feng K, Li J, Yu D, Fan Q, Tang T, et al. Curcumin inhibits apoptosis of chondrocytes through activation ERK1/2 signaling pathways induced autophagy. Nutrients 2017;9(4):414.
[63] Liu J, Liu W, Lu Y, Tian H, Duan C, Lu L, et al. Piperlongumine restores the balance of autophagy and apoptosis by increasing BCL2 phosphorylation in rotenone-induced Parkinson disease models. Autophagy 2018;14(5). 845-61.
[64] Saatci Ö, Borgoni S, Akbulut Ö, Durmuş S, Raza U, Eyüpoğlu E, et al. Targeting PLK1 overcomes T-DM1 resistance via CDK1-dependent phosphorylation and inactivation of Bcl-2/xL in HER2-positive breast cancer. Oncogene 2018;37(17). 2251-69.
[65] Maejima Y, Kyoi S, Zhai P, Liu T, Li H, Ivessa A, et al. Mst1 inhibits autophagy by promoting the interaction between Beclin1 and Bcl-2. Nat Med 2013;19(11). 1478-88.